

quantum efficiencies of Table I are averaged values over a pH range between 3 and 2 and their accuracy is $\pm 20\%$. Nevertheless, because in all of our measurements the change in pH has been the same, the relative quantum efficiencies are quite accurate.

Acknowledgment. We thank Prof. James R. Brock and Prof. John G. Ekerdt for useful discussions and Mrs. Maya Nair for

competent assistance. This work was supported by the Division of advanced Energy Projects, Office of Basic Energy Sciences, U.S. Department of Energy, under Contract DE-FG05-90ER12101-A0002.

Registry No. CH₃OH, 67-56-1; Pd, 7440-05-3; TiO₂, 13463-67-7; O₂, 7782-44-7; sodium 2,2-dichloropropionate, 127-20-8.

Characterization of the Energy Surface for the Oxidative Addition of Silanes to CpMn(CO)₂(heptane)

Dennis M. Hester, Jiemin Sun, Aaron W. Harper, and Gilbert K. Yang*

Contribution from the Department of Chemistry, University of Southern California, Los Angeles, California 90089-0744. Received November 13, 1991

Abstract: The energetic surface for the oxidative addition reaction of silanes to CpMn(CO)₂(heptane) (**2**) has been studied by a combination of photoacoustic calorimetry and variable-temperature kinetic studies. For seven different silanes the enthalpy for the oxidative addition reaction, ΔH_{-1} , ranged from -22.1 to -13.5 kcal/mol. ΔH_{-1} was found to depend both on the electron donating ability of the silane as well as on the cone angle of the silane. A threshold cone angle of 135° must be reached before the steric effects turn on. The rate constants for the oxidative addition reactions at 25°C were all similar, ca. 2.5×10^6 L/(mol·s), indicative of an early transition state where steric and electronic effects have not yet manifested themselves. Kinetic studies of the reductive elimination of Et₃SiH from CpMn(CO)₂(H)(Et₃Si) are consistent with a mechanism involving a pre-equilibrium step with the reactive intermediate **2** which is then trapped by PPh₃. The activation parameters are the following: $\Delta H_1^\ddagger = 27.4 \pm 0.8$ kcal/mol and $\Delta S_1^\ddagger = 11.5 \pm 2.5$ eu. The values for ΔH_{-1}^\ddagger determined by Wrighton and the results of ΔH_1^\ddagger and ΔH_{-1} reported here are consistent with one another. Trapping of the CpMn(CO)₂(heptane) intermediate is favored by PPh₃ over Et₃SiH with $\Delta\Delta H^\ddagger = -2.1 \pm 0.5$ kcal/mol and $\Delta\Delta S^\ddagger = -2.7 \pm 1.0$ eu. From the values of ΔH_{-1}^\ddagger and ΔH_1^\ddagger , the strength of the Mn–heptane interaction is estimated to be 8 kcal/mol.

The oxidative addition of alkylsilanes to transition-metal complexes has been the focus of much recent attention.¹ This reaction plays an integral role in the hydrosilation of olefins and serves as an important model for understanding analogous C–H activation reactions. The bonding in metal silyl hydride complexes varies in description from being a relatively weak η^2 -silane–metal interaction at one extreme to the stronger oxidative addition interaction found in a true metal silyl hydride moiety. From the relative rates of reductive elimination of Cl₃SiH and Ph₃SiH from the corresponding CpMn(CO)₂(H)(SiR₃) complexes, Graham and Hart-Davis² concluded that “Cl₃SiH is much more firmly attached” to the complex than is Ph₃SiH. This observation is now understood to be a result of more advanced Si–H bond cleavage with the more electron deficient Cl₃SiH. Data from single-crystal X-ray and neutron diffraction analyses³ and UV photoelectron spectra⁴ support the conclusion that the interaction of the silane with the Mn center more closely approaches complete oxidative addition when more electron withdrawing substituents are on the silane. These results are also supported by theoretical studies which show that an important component of the silane–metal interaction is π -back-bonding from the CpMn(CO)₂ moiety to

the Si–H σ^* orbital.⁵ Electron-withdrawing substituents on the silane will lead to a stronger silane–metal interaction.

In contrast, Zhang, Dobson, and Brown⁶ have published recent work which suggests that more electron donating substituents on the silane result in stronger Cr–silane interactions. This result is thought to be a consequence of the greater role of σ -donation from the silane to the electrophilic Cr(CO)₅ center (in comparison to CpMn(CO)₂). These workers also found that the rate of the reductive elimination of silane from (CO)₅Cr(H)(SiRR'₂) could be described as a function of both the electron donating ability and the cone angle of the corresponding phosphine.

Comparatively little is known about how the steric requirements of the silane influence the nature of the metal–silane interaction in the CpMn(CO)₂(H)(SiR₃) system. Wrighton and Hill have reported kinetic studies of the oxidative addition reaction of silanes to CpMn(CO)₂ in hydrocarbon solution.⁷ A slight dependence on the steric bulk of the silane was found. In this paper we present studies of the heat of reaction of coordinatively unsaturated CpMn(CO)₂(heptane) with silanes of differing steric bulk. A strong dependence on steric bulk is found for silanes exceeding a “steric threshold”, but little effect is seen for smaller silanes. The kinetics of both the oxidative addition process and the reductive elimination process are discussed in the context of the enthalpy of reaction. The stabilization of the CpMn(CO)₂ moiety by the heptane solvent can be inferred from these data. Together, a complete picture of the Mn–silane energy profile is presented.

Experimental Section

General. Ferrocene (Aldrich) was sublimed before use and CpMn(CO)₃ (Strem) was recrystallized prior to use. Heptane was distilled

(1) For a recent review see: Schubert, U. *Adv. Organomet. Chem.* **1990**, *30*, 151–187.

(2) Hart-Davis, A. J.; Graham, W. A. G. *J. Am. Chem. Soc.* **1971**, *93*, 4388–4393.

(3) (a) Schubert, U.; Scholz, G.; Müller, J.; Ackermann, K.; Worle, B.; Stansfield, R. F. D. *J. Organomet. Chem.* **1986**, *306*, 303. (b) Graham, W. A. G. *J. Organomet. Chem.* **1986**, *300*, 81. (c) Carré, F.; Colomer, E.; Corriu, R. J. P.; Vioux, A. *Organometallics* **1984**, *3*, 1272. (d) Graham, W. A. G.; Bennett, M. J. *Chem. Eng. News* **1970**, *48*(24), 75. (e) Schubert, U.; Ackermann, K.; Worle, B. *J. Am. Chem. Soc.* **1982**, *104*, 7378. (f) Schubert, U.; Ackermann, K.; Kraft, G.; Worle, B. *Z. Naturforsch. B: Anorg. Chem. Org. Chem.* **1983**, *38*, 1488.

(4) (a) Lichtenberger, D. L.; Rai-Chaudhuri, A. *J. Am. Chem. Soc.* **1989**, *111*, 3583. (b) Lichtenberger, D. L.; Rai-Chaudhuri, A. *J. Am. Chem. Soc.* **1990**, *112*, 2492. (c) Lichtenberger, D. L.; Rai-Chaudhuri, A. *Inorg. Chem.* **1990**, *29*, 975.

(5) Rabaã, H.; Saillard, J.-Y.; Schubert, U. *J. Organomet. Chem.* **1987**, *330*, 397–413.

(6) Zhang, S.; Dobson, G. R.; Brown, T. L. *J. Am. Chem. Soc.* **1991**, *113*, 6908–6916.

(7) Hill, R. H.; Wrighton, M. S. *Organometallics* **1987**, *6*, 632–638.

Table I. Enthalpic and Kinetic Data for the Photolysis of $\text{CpMn}(\text{CO})_3$ in Heptane Solutions of Silanes According to Scheme 1^a

silane ^b	$\text{CpMn}(\text{CO})_3$ $\Delta H_{\text{Mn-CO}}$ (kcal/mol)	ΔH_{-1} (kcal/mol)	$10^{-6}k_{-1}$ (L/(mol·s))	$10^{-6}k_{-1} \pm 10\%$ (L/(mol·s)) lit. value ^c	cone angle θ^d (deg)	χ^e (cm ⁻¹)
(<i>n</i> -hex) ₃ SiH ₃	46.9 ± 1.8	-22.1 ± 1.5	3.6 ± 0.5		102 ^f	12.85
EtMe ₂ SiH	48.3 ± 1.2	-20.2 ± 1.5	2.5 ± 0.8	5.6	123 ^f	7.8
Et ₃ SiH	46.7 ± 2.1	-20.1 ± 2.1	2.5 ± 0.5	3.1	132	6.3
<i>n</i> -Pr ₃ SiH	46.5 ± 2.0	-19.7 ± 1.9	2.3 ± 0.4	2.3	132	5.78
(<i>n</i> -hex) ₃ SiH	45.6 ± 3.0	-19.1 ± 1.6	2.1 ± 0.4		132	5.25
(<i>i</i> -Bu) ₃ SiH	46.5 ± 1.8	-17.3 ± 1.8	1.8 ± 0.2		143	5.7
(<i>i</i> -Pr) ₃ SiH	47.2 ± 1.7	-13.5 ± 1.7	2.6 ± 0.5	2.6	160	3.45
average	46.8 ± 2.1					

^a Errors are given as one standard deviation of the scatter in the data. The error on the average is the pooled standard deviation of 79 determinations. ^b *n*-hex = *n*-C₆H₁₃; *i*-Bu = *i*-C₄H₉; *n*-Pr = *n*-C₃H₇; *i*-Pr = *i*-C₃H₇. ^c Calculated from the data in ref 7. ^d Reference 16. ^e Reference 18. ^f Calculated from the cone angles of PR'₃ and PR''₃ using $\theta = 1/3\theta' + 2/3\theta''$.

forming the corresponding $\text{CpMn}(\text{CO})_2(\text{H})(\text{SiR}_3)$ complex (1). From the photoacoustic signal the enthalpy of substitution of CO by heptane ($\Delta H_{\text{Mn-CO}}$) and the enthalpy of the subsequent oxidative addition process (ΔH_{-1}) are determined. The k_{obsd} for displacement of heptane by silane is also found. The second-order rate constant k_{-1} for the silane oxidative addition is obtained from the plot of k_{obsd} vs [silane]. Both the enthalpic and kinetic results are listed in Table I.

Mn-CO Bond Dissociation. Since the photochemically induced dissociation of CO from $\text{CpMn}(\text{CO})_3$ is not dependent on the presence of silane in solution, $\Delta H_{\text{Mn-CO}}$ is expected to be independent of the silane. Indeed, for the seven different silanes reported in Table I, the corresponding values for $\Delta H_{\text{Mn-CO}}$ agree with one another within experimental error and average 46.8 ± 2.1 kcal/mol. This average value is in excellent agreement with our previously reported value of 46.7 ± 1.7 kcal/mol for this process in the presence of two-electron donors such as THF, *cis*-cyclooctene, acetone, and Bu₂S.¹⁰

The enthalpy represented by $\Delta H_{\text{Mn-CO}}$ is the heat of exchange of a CO ligand from $\text{CpMn}(\text{CO})_3$ for a molecule of heptane. Presuming that there is some stabilization of the $\text{CpMn}(\text{CO})_2$ moiety by the heptane ligand, a lower bound of 46.8 kcal/mol can be set on the gas-phase bond dissociation energy of CO from $\text{CpMn}(\text{CO})_3$.

Steric Effects on the Enthalpy of Oxidative Addition of Silanes to $\text{CpMn}(\text{CO})_2(\text{heptane})$. In our effort to probe the steric effects in the oxidative addition of silanes to the $\text{CpMn}(\text{CO})_2$ moiety, two considerations were important. The first was the need to minimize differences, and the corresponding effect on ΔH_{-1} , in the electronic character of the silanes. This could be best accomplished by examination of a series of silanes with electronically similar substituents. The second was to keep the possible sites of reactivity limited to just the Si-H moiety. There is much evidence for the ability of coordinatively unsaturated metal complexes to coordinate to arene rings, halogen substituents, and other functional groups.¹⁵ Although attack on such a remote functional group may eventually lead to the expected silane activation product, this rearrangement process may be sufficiently slow to complicate the reaction scheme. Since the photoacoustic calorimetry experiment is sensitive to the kinetics of reactions,

(15) For examples of complexes containing the η^2 -arene moiety see: (a) Brauer, D. J.; Krüger, C. *Inorg. Chem.* **1977**, *16*, 884-891. (b) Sweet, J. R.; Graham, W. A. G. *J. Am. Chem. Soc.* **1983**, *105*, 305-306. (c) Jones, W. D.; Feher, F. J. *J. Am. Chem. Soc.* **1984**, *106*, 1650-1663. (d) Allegra, G.; Tettamanti Cassagrande, G.; Immirzi, A.; Porri, L.; Vitulli, G. *J. Am. Chem. Soc.* **1970**, *92*, 289-293. (e) Davis, R. E.; Pettit, R. *J. Am. Chem. Soc.* **1970**, *92*, 176-177. (f) Browning, J.; Green, M.; Penfold, B. R.; Spencer, J. L.; Stone, F. G. A. *J. Chem. Soc., Chem. Commun.* **1973**, 31-32. For examples of complexes containing halocarbon-metal interactions see: (g) Newbound, T. D.; Colman, M. R.; Miller, M. M.; Wulfsberg, G. P.; Anderson, O. P.; Strauss, S. H. *J. Am. Chem. Soc.* **1989**, *111*, 3762-3764. (h) Winter, C. H.; Arif, A. M.; Gladysz, J. M. *J. Am. Chem. Soc.* **1987**, *109*, 7560-7561. (i) Fernandez, J. M.; Gladysz, J. A. *Organometallics* **1989**, *8*, 207-219. (j) Beck, W.; Schloter, K. *Z. Naturforsch.* **1978**, *33B*, 1214. (k) Cook, P. M.; Dahl, L. F.; Dickerdorf, D. W. *J. Am. Chem. Soc.* **1972**, *94*, 5511-5513. (l) Burk, M. J.; Crabtree, R. H.; Holt, E. M. *Organometallics* **1984**, *3*, 638-640. (m) Burk, M. J.; Segmüller, B.; Crabtree, R. H. *Organometallics* **1987**, *6*, 2241-2246. (n) Crabtree, R. H.; Fallor, J. W.; Mellea, M. F.; Quirk, J. M. *Organometallics* **1982**, *1*, 1361-1366.

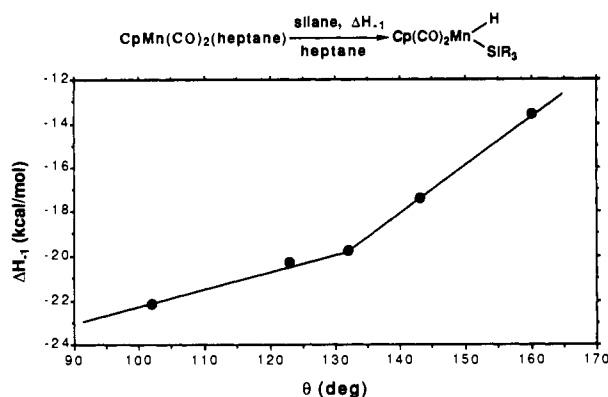


Figure 1. Plot of ΔH_{-1} vs θ for the oxidative addition of silanes to $\text{CpMn}(\text{CO})_2(\text{heptane})$ in heptane solution at 298 K. For clarity, the point at $\theta = 132^\circ$ is the average of values obtained for three silanes.

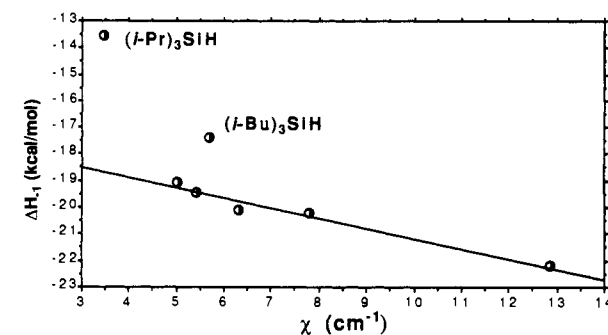


Figure 2. Plot of ΔH_{-1} versus χ . The linear least-squares fit for the smaller silane ligands is shown with $\Delta H_{-1} = -0.371\chi - 17.431$ and $r^2 = 0.971$.

this complication would affect the data if the rate constants for the rearrangement are slower than 10^7 s^{-1} . We chose to minimize these potential complications by studying only the trialkylsilanes and *n*-hexylsilane as listed in Table I.

The cone angles θ for these silanes were estimated to be identical to Tolman's cone angles for the corresponding phosphines.¹⁶ Brown et al. have taken a similar approach in examination of steric and electronic effects in silane oxidative addition to $\text{Cr}(\text{CO})_5$.⁶ When the cone angles of phosphines such as PR''₂ were unavailable, the cone angle of the silane was calculated from the cone angles of PR'₃ and PR''₃ using $\theta = 1/3\theta' + 2/3\theta''$.

The results of the photoacoustic calorimetry experiments on the enthalpy of oxidative addition of the silanes to $\text{CpMn}(\text{CO})_2(\text{heptane})$ (2) shown in Scheme 1 are given in Table I. A plot of ΔH_{-1} vs θ is given in Figure 1. The enthalpies of oxidative addition range from -22.1 kcal/mol for *n*-hexylsilane to -13.5 kcal/mol for the bulkier triisopropylsilane. The other silanes fall somewhere in between these extremes. It is important to note that ΔH_{-1} incorporates both the enthalpy of dissociation of heptane

(16) Tolman, C. A. *Chem. Rev.* **1977**, *77*, 313-348.

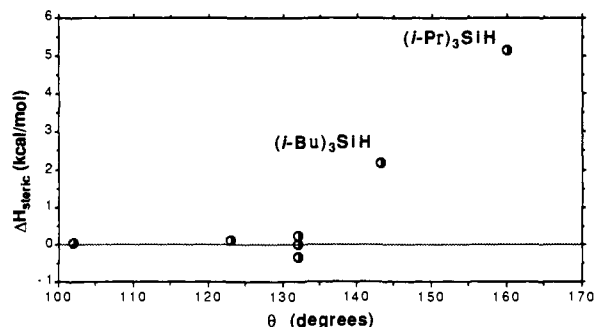


Figure 3. Plot of ΔH_{steric} versus θ showing a steric threshold at $\sim 135^\circ$.

and the enthalpy of oxidative addition of silane. Therefore the enthalpy of oxidative addition of silanes to *unsolvated* CpMn(CO)₂ would be more exothermic by the degree of heptane-Mn stabilization (vide infra).

From Figure 1, it is clear that as the cone angle increases from 102° to 135° there is only a slight decrease in the exothermicity of the oxidative addition reaction. However, as θ increases beyond $\sim 135^\circ$, ΔH_{-1} rapidly decreases in magnitude. Such a sudden change in the dependence of the ΔH_{-1} on the cone angle may be interpreted in the context of a "steric threshold" as has been discussed by Giering et al.¹⁷

The small slope in the data at cone angles less than $\sim 135^\circ$ may be caused by slight differences in the electron donating abilities of the different silyl groups. Giering et al.¹⁷ have separated steric from electronic contributions to reaction enthalpies and reaction kinetics. In analogous fashion, we may determine the purely steric contribution to ΔH_{-1} provided with a reasonable estimate of the silane electron donor ability. Since there is little information on the donating ability of silyl groups to metal centers, the donating abilities, χ (Table I), of the analogous phosphine ligands were used.¹⁸ A plot of ΔH_{-1} versus χ (Figure 2) shows that the silanes with cone angle less than 135° fit on a straight line defined by

$$\Delta H_{-1} = -0.371\chi - 17.431 \quad (3)$$

The sterically demanding (*i*-Bu)₃SiH and (*i*-Pr)₃SiH show considerable deviation from this line. The deviation from the line (ΔH_{steric}) is due to steric demands of the silyl groups. A plot of ΔH_{steric} versus θ (Figure 3) then gives the dependence of steric effects on the cone angle. Clearly, steric effects are not significant until a threshold angle of 135° is reached. For the slightly bulky (*i*-Bu)₃SiH, ΔH_{steric} is only ~ 2 kcal/mol. For the larger (*i*-Pr)₃SiH, ΔH_{steric} is more than 5 kcal/mol. Consequently, steric demands *reduce* ΔH_{-1} for these two silanes, respectively, by 2 and 5 kcal/mol from what would be expected based solely on electronic considerations.¹⁹

Kinetics of the Oxidative Addition of Silanes to CpMn(CO)₂(heptane). The second-order rate constants k_{-1} for the silane oxidative addition reactions were obtained as the slope of plots of k_{obsd} vs [silane]. Examples of these plots are given in Figure 4, and the data are tabulated in Table I. The data for all the silanes give excellent linear plots with the best fit line passing through the origin. Although three orders of magnitude slower than diffusion controlled, all these reactions are quite fast, $k_{-1} \approx 10^6$ L/(mol·s), and vary by only a factor of 2 from the fastest ((*n*-hex)SiH₃) to the slowest (*i*-Bu₃SiH). However, since (*n*-hex)SiH₃ has three sites for oxidative addition to a Si-H bond, simple statistical arguments would predict k_{-1} for this silane would be faster than k_{-1} for the trialkylsilanes. The six trialkylsilanes

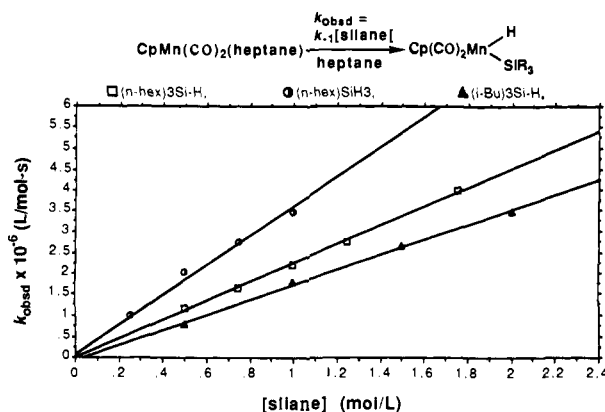
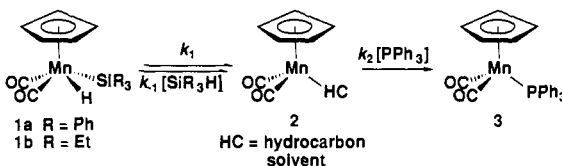


Figure 4. Plots of k_{obsd} vs [silane] for oxidative addition of silanes to CpMn(CO)₂(heptane) at 298 K: for (*n*-hex)SiH₃ (open squares), $k_{-1} = 3.6 \pm 0.5 \times 10^6$ L/(mol·s), $r^2 = 0.992$; for (*n*-hex)₃SiH (half-circles), $k_{-1} = 2.1 \pm 0.4 \times 10^6$ L/(mol·s), $r^2 = 0.998$; for (*i*-Bu)₃SiH (solid triangles), $k_{-1} = 1.8 \pm 0.2 \times 10^6$ L/(mol·s), $r^2 = 0.998$.

Scheme II



studied all exhibit second-order rate constants which are within experimental error of one another. The similarity of these rate constants suggests that the transition state for the oxidative addition reaction is very early with very little Mn-silane interaction. Consequently, k_{-1} is not significantly influenced by the steric bulk of the silane.

Wrighton and Hill have reported low-temperature studies of the kinetics of oxidative addition of silanes to CpMn(CO)₂ generated in Et₃SiH and 3-methylpentane solution.⁷ From their data for the reaction of triethylsilane with CpMn(CO)₂(hydrocarbon) we calculate $\Delta H_{-1}^\ddagger = 7.8$ kcal/mol and $\Delta S_{-1}^\ddagger = -2.4$ eu.²⁰ From these activation parameters, the rate constant expected for the corresponding reaction at 298 K is calculated to be 3.1×10^6 L/(mol·s). This value agrees well with our value of 2.5×10^6 L/(mol·s) for the same reaction. Wrighton and Hill used competition experiments between Et₃SiH and other silanes to determine the corresponding rate constants k_{-1} for those silanes. For comparison, these results are given in Table I. Although there is some disagreement for the values of k_{-1} for Me₂EtSiH, the overall agreement with our independent rate constant determinations is excellent.

Kinetic Studies of the Reductive Elimination of Et₃SiH from CpMn(CO)₂(H)(SiEt₃). Graham and Hart-Davis have studied the substitution of Ph₃SiH from CpMn(CO)₂(H)(SiPh₃) (1a) by PPh₃ in heptane solution.² Their kinetic data supported a mechanism involving reversible reductive elimination of silane followed by uptake of PPh₃ (Scheme II).

From the mechanism in Scheme II, the kinetic expressions in eqs 4 and 5 are found by applying the steady state approximation to the heptane-coordinated intermediate 2.

$$k_{\text{obsd}} = \frac{k_1 k_2 [\text{PPh}_3]}{k_{-1} [\text{R}_3\text{SiH}] + k_2 [\text{PPh}_3]} \quad (4)$$

$$\frac{1}{k_{\text{obsd}}} = \frac{1}{k_1} + \frac{k_{-1} [\text{R}_3\text{SiH}]}{k_1 k_2 [\text{PPh}_3]} \quad (5)$$

It seems reasonable that a similar mechanism would be in effect for the reductive elimination of Et₃SiH from complex 1b. Since

(17) (a) Rahman, Md. M.; Liu, H.; Eriks, K.; Prock, A.; Giering, W. P. *Organometallics* **1989**, *8*, 1-7. (b) Golovin, M. N.; Rahman, Md. M.; Belmonte, J. E.; Giering, W. P. *Organometallics* **1985**, *4*, 1981-1991. (c) Liu, H.-Y.; Eriks, K.; Prock, A.; Giering, W. P. *Organometallics* **1990**, *9*, 1758-1766. (d) Rahman, Md. M.; Liu, H.-Y.; Prock, A.; Giering, W. P. *Organometallics* **1987**, *6*, 650-658.

(18) Bartik, T.; Himmler, T.; Schulte, H.-G.; Seevogel, K. *J. Organomet. Chem.* **1984**, *272*, 29-41.

(19) Overall, ΔH_{-1} can be calculated using a piecewise function: For $\theta < 135^\circ$, $\Delta H_{-1} = -0.371\chi - 17.431$. For $\theta > 135^\circ$, $\Delta H_{-1} = -0.371\chi + 0.186\theta - 42.0$.

(20) From their kinetic data, Wrighton and Hill⁷ reported values of $\Delta H_{-1}^\ddagger = 7.2 \pm 1.0$ kcal/mol and $\Delta S_{-1}^\ddagger = -6.7 \pm 2.4$ eu. From the same data, we obtain $\Delta H_{-1}^\ddagger = 7.8$ kcal/mol and $\Delta S_{-1}^\ddagger = -2.4$ eu through computer-generated linear least-squares analysis. We believe the disagreement between these two sets of values is simply a result of differences in the methods of graphical analysis used.

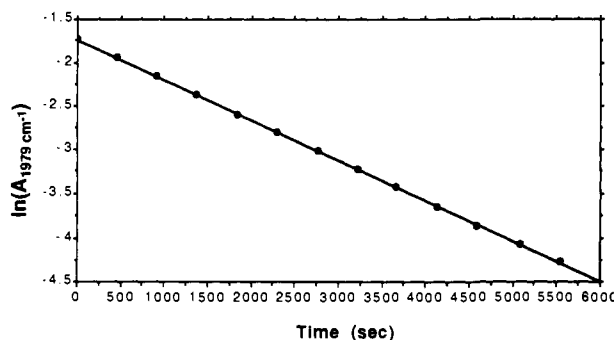


Figure 5. Pseudo-first-order rate plot for the reaction of CpMnH(SiEt₃)(CO)₂ with PPh₃ in *n*-heptane at 50.0 °C: [PPh₃] = 14.8 mM, [HSiEt₃] = 26.4 mM, [CpMnH(SiEt₃)(CO)₂] = 1.6 mM; $k_{\text{obsd}} = 4.59 \times 10^{-4} \text{ s}^{-1}$; $r^2 = 1.000$.

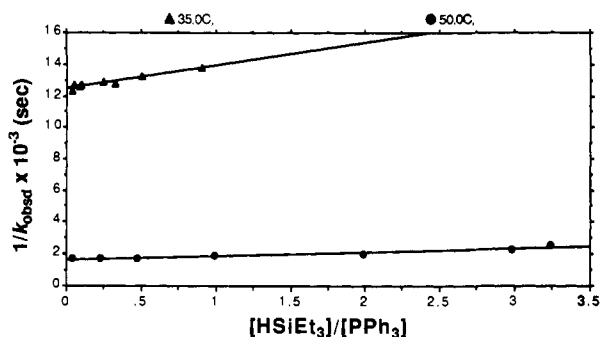


Figure 6. Plot of $1/k_{\text{obsd}}$ versus the relative concentrations of [HSiEt₃] and [PPh₃] for the reaction of CpMnH(SiEt₃)(CO)₂ and PPh₃. The square points represent data taken at 35.0 °C. The round points represent data taken at 50.0 °C. The derived values of k_1 , k_2/k_{-1} , and r^2 are given in Table II.

the k_1 step is the reverse of the k_{-1} step examined via photoacoustic calorimetry, we examined the enthalpy of activation for this process to provide additional information about the energetics of the silane-metal interactions.

Reductive elimination of Et₃SiH from CpMn(CO)₂(H)(SiEt₃) (**1b**) readily occurs from the solid at room temperature, making this complex difficult to isolate. Wrighton and Hill have reported the ¹H NMR and IR characterization of CpMn(CO)₂(H)(SiEt₃) but did not report its isolation.⁷ As a consequence, we performed kinetic studies on heptane solutions of CpMn(CO)₂(H)(SiEt₃) prepared by photolysis of heptane solutions of CpMn(CO)₃ in the presence of a large excess of Et₃SiH. These solutions were diluted with heptane and then PPh₃ and Et₃SiH were added to the desired concentration. The reductive elimination reactions at 35–80 °C were monitored by the disappearance of the band at 1979 cm⁻¹ in the IR spectrum attributed to CpMn(CO)₂(H)(SiEt₃). The bands at 1946 and 1885 cm⁻¹, corresponding to phosphine complex **3**, were observed to simultaneously grow in. For the decrease in the absorbance of the starting material, plots of ln *A* vs time exhibited good pseudo-first-order kinetics as shown in Figure 5.

The dependence of k_{obsd} on the concentrations of PPh₃ and Et₃SiH agreed well with the mechanism for silane reductive elimination proposed by Graham and Hart-Davis illustrated in Scheme II.² For this mechanism eq 5 predicts that $1/k_{\text{obsd}}$ will be linearly dependent on [Et₃SiH]/[PPh₃]. Over the temperature range of 35–80 °C, the reciprocal plots of $1/k_{\text{obsd}}$ vs [Et₃SiH]/[PPh₃] (Figures 6 and 7) gave excellent straight lines with slope k_{-1}/k_1k_2 and with $1/k_1$ as the *y* intercept. The values of k_1 and k_2/k_{-1} derived from these plots are summarized in Table II.

Figure 8 shows a plot of k_{obsd} vs [PPh₃] with [Et₃SiH] = 0.025 M at 50 °C. The plot clearly exhibits saturation kinetics for concentrations of phosphine >0.02 M. This is consistent with trapping of heptane complex **2** by phosphine faster than trapping by Et₃SiH. The data are closely fit by a plot of k_{obsd} (calculated from eq 5 using the values of k_1 and k_2/k_{-1} from Table II and [Et₃SiH] = 0.025 M) vs [PPh₃]. None of the data illus-

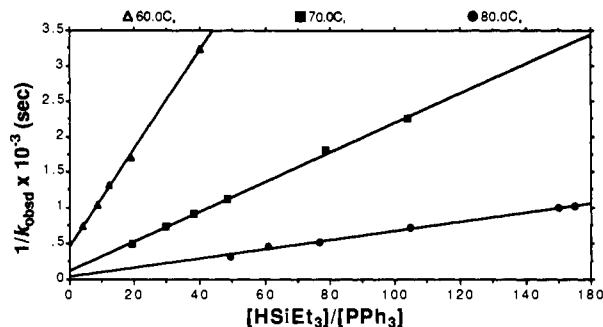


Figure 7. Plot of $1/k_{\text{obsd}}$ versus the relative concentrations of [HSiEt₃] and [PPh₃] for the reaction of CpMnH(SiEt₃)(CO)₂ and PPh₃. The open triangles represent data taken at 60.0 °C. The square points represent data recorded at 70.0 °C. The round points represent data recorded 80.0 °C. The derived values of k_1 , k_2/k_{-1} , and r^2 are given in Table II.

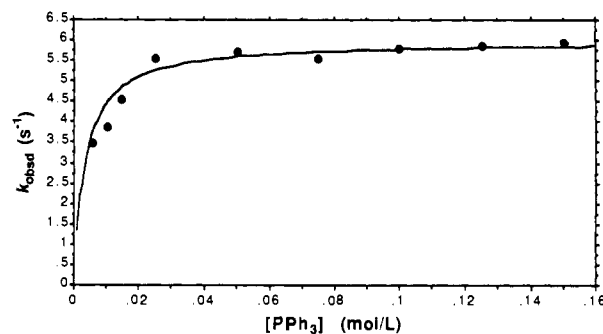


Figure 8. Plot of k_{obsd} vs [PPh₃] at 50 °C: [Et₃SiH] = 0.025 M. The fitted curve is a plot of k_{obsd} (calculated from eq 5 using the values of k_1 and k_2/k_{-1} from Table II and [Et₃SiH] = 0.025 M) vs [PPh₃].

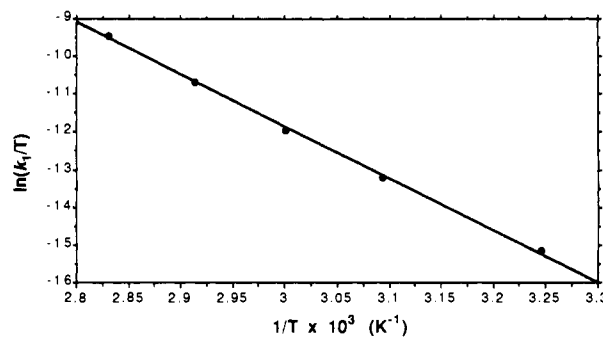


Figure 9. Eyring plot of $\ln(k_1/T)$ vs $1/T$: $\Delta H_1^\ddagger = 27.4 \pm 0.8 \text{ kcal/mol}$ and $\Delta S_1^\ddagger = 11.5 \pm 2.5 \text{ eu}$; $r^2 = 0.999$.

Table II. Rate Constants and Rate Constant Ratios Derived from the Plots Shown in Figures 6 and 7

temp (°C)	$10^4 k_1$ (s ⁻¹)	k_2/k_{-1}	r^2
35.0	0.802	8.6	0.933
50.0	5.97	7.3	0.915
60.0	21.8	6.6	0.999
70.0	79.7	6.0	0.998
80.0	280	5.5	0.995

trated in Figure 8 were used in the derivation of either k_1 or k_2/k_{-1} , thus giving an independent confirmation of the rate model.

The activation parameters for the reductive elimination of Et₃SiH from **1b** were determined from the Eyring plot of $\ln(k_1/T)$ vs $1/T$ (Figure 9). A good linear fit was obtained over the 35–80 °C temperature range yielding $\Delta H_1^\ddagger = 27.4 \pm 0.8 \text{ kcal/mol}$ and $\Delta S_1^\ddagger = 11.5 \pm 2.5 \text{ eu}$. The moderately positive entropy of activation is suggestive of a largely dissociative transition state in the reductive elimination reaction. In comparison, Graham and Hart-Davis determined the activation parameters for the elimination of Ph₃SiH from **1a** to be $\Delta H_1^\ddagger = 29.2 \pm 0.3 \text{ kcal/mol}$ and $\Delta S_1^\ddagger = 16.3 \pm 1.0 \text{ eu}$.² The greater thermal reactivity of **1b** in

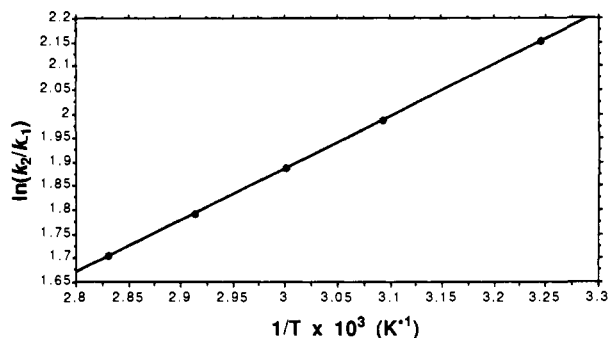


Figure 10. Plot of $\ln(k_2/k_{-1})$ vs $1/T$: $\Delta\Delta H^\ddagger = -2.1 \pm 0.5$ kcal/mol and $\Delta\Delta S^\ddagger = -2.7 \pm 1.0$ eu; $r^2 = 1.000$.

comparison to **1a** is consistent with these values.

The ratios of k_2/k_{-1} clearly show that trapping of the heptane complex **2** by PPh_3 is faster than trapping by Et_3SiH . The slight temperature dependence of k_2/k_{-1} is illustrated in a plot of $\ln(k_2/k_{-1})$ vs $1/T$. An excellent linear plot was obtained from which $\Delta\Delta H^\ddagger = -2.1 \pm 0.5$ kcal/mol and $\Delta\Delta S^\ddagger = -2.7 \pm 1.0$ eu are obtained (Figure 10). With very similar entropies of activation, the faster trapping by PPh_3 is due solely to 2-kcal/mol stabilization of the transition state by the incoming phosphine ligand.

Discussion

The enthalpy of oxidative addition, ΔH_{-1} , of the five smaller silanes to $\text{CpMn}(\text{CO})_2(\text{heptane})$ exhibited a good linear dependence on χ as given by eq 3. Owing to their smaller size, the observation of a good fit to the single variable χ suggests that for these silanes steric contributions to ΔH_{-1} are small. The excellent fit of the values for ΔH_{-1} to the χ value for the corresponding phosphines indicates that the same factors which govern the electron donating ability of the phosphines also govern the donating ability of the silanes. The steric component to ΔH_{-1} for the larger (*i*-Bu) $_3\text{SiH}$ and (*i*-Pr) $_3\text{SiH}$ is determined from the deviation of the actual enthalpy of reaction from the predicted values using eq 3. The deviation corresponds to a steric influence of 2 and 5 kcal/mol, respectively, on ΔH_{-1} . These data give a threshold of 135° for the onset of steric effects. The steric threshold for the oxidative addition of silanes to the $\text{CpMn}(\text{CO})_2$ moiety suggests that the vacant coordination site on the metal center can accommodate silanes such as Et_3SiH with cone angles up to $\sim 135^\circ$ without difficulty. As the cone angle of the silane exceeds this threshold θ , the silane becomes too large to easily fit into the pocket defined by the steric bulk of the other ligands around the metal center. This causes the exothermicity of oxidative addition reaction to markedly decrease as θ continues to increase.

It is interesting to note that Et_3SiH , (*n*-Pr) $_3\text{SiH}$, and (*n*-hex) $_3\text{SiH}$ all display values of ΔH_{-1} which, while similar, are somewhat different. The differences are within experimental error but seem to suggest a slightly greater steric effect as the alkyl chain increases from ethyl to *n*-propyl to *n*-hexyl. This may be indicative that the true cone angles of all three silanes is not identical.

Examination of the crystal structure of $\text{CpMn}(\text{CO})_2\text{PPh}_3$ shows that the $\text{CpMn}(\text{CO})_2$ moiety has a pocket large enough to accommodate phosphines with a cone angle up to 145° without significant perturbation.²¹ In comparison, the molecular structure of $\text{CpMn}(\text{CO})_2(\text{H})(\text{SiPh}_3)$ shows significant, though slight indications that the $(\text{H})(\text{SiPh}_3)$ ligands are more sterically demanding than is PPh_3 .^{3b,d} In particular, the smaller of the two Si-Mn-CO angles is 80.4° . This is 10° smaller than the smallest P-Mn-CO angle in $\text{CpMn}(\text{CO})_2\text{PPh}_3$. This brings the SiPh_3 group closer to the CO, effectively reducing the pocket size on the metal center. As a consequence, the steric threshold for silanes is expected to be considerably smaller than that for phosphines.

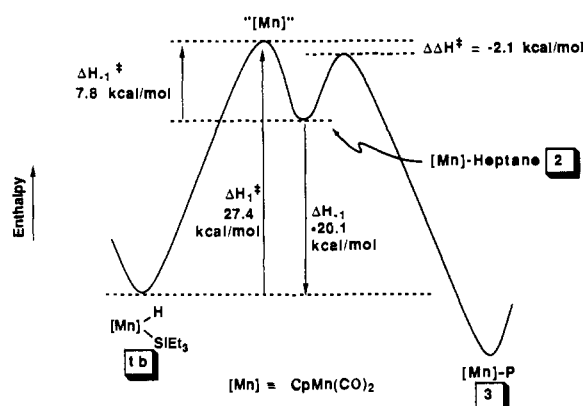


Figure 11. Relative enthalpy diagram for the interconversion of $\text{CpMn}(\text{CO})_2(\text{H})(\text{SiEt}_3)$ (**1b**), $\text{CpMn}(\text{CO})_2(\text{heptane})$ (**2**), and $\text{CpMn}(\text{CO})_2(\text{PPh}_3)$ (**3**).

The studies of Wrighton and Hill on the oxidative addition Et_3SiH to $\text{CpMn}(\text{CO})_2$ were performed either in neat Et_3SiH or in 3-methylpentane solution.⁷ Assuming that the stabilization of $\text{CpMn}(\text{CO})_2$ in these solvents is identical to its stabilization in heptane solution, then Wrighton's results can be discussed together with those reported here. For the oxidative addition reaction of Et_3SiH to heptane solvate **2** yielding complex **1b** (Scheme II), the enthalpy of reaction can be calculated as the difference of the enthalpies of activation for the oxidative addition reaction and the reductive elimination reaction, i.e. $\Delta H_{-1} = \Delta H_{1,1}^\ddagger - \Delta H_{1,2}^\ddagger$ (Figure 11). From Wrighton's results, displacement of hydrocarbon from $\text{CpMn}(\text{CO})_2(\text{HC})$, the k_{-1} step in Scheme II, has a small activation enthalpy ΔH_{-1}^\ddagger of 7.8 kcal/mol. From the kinetic results reported herein, the activation enthalpy $\Delta H_{1,1}^\ddagger$ for the reductive elimination of Et_3SiH from **1b** is 27.4 kcal/mol (Figure 11). Thus, the enthalpy of reaction for oxidative addition of Et_3SiH to $\text{CpMn}(\text{CO})_2(\text{heptane})$ is calculated to be $\Delta H_{-1} = -19.6$ kcal/mol. This is in excellent agreement with the experimentally determined value of $\Delta H_{-1} = -20.1$ kcal/mol from the photoacoustic calorimetric results. The agreement in these values obtained through very different experimental methods is very supportive of the accuracy of these determinations.

The disagreement between the previously reported value for $\Delta H_{-1} = -13.8$ kcal/mol^{9j} and our value of -20.1 kcal/mol is probably due to the relatively slow reaction of $\text{CpMn}(\text{CO})_2(\text{HC})$ with Et_3SiH . As demonstrated by Wrighton, the oxidative addition reaction of Et_3SiH to solvate **2** appears to obey the same kinetics regardless of whether the solvent is Et_3SiH or 3-methylpentane.⁷ Therefore, the pseudo-first-order rate constant $k_{\text{neat silane}}$ for the oxidative addition of Et_3SiH to **2** in neat (6.26 M) Et_3SiH can be calculated to be $k_{\text{neat silane}} = k_{-1}[\text{Et}_3\text{SiH}] = 1.9 \times 10^7 \text{ s}^{-1}$. This rate is in the time regime slow enough to be detected by the photoacoustic experiment. Failure to consider the oxidative addition as a slow reaction will lead to an underestimate of ΔH_{-1} .

The trapping of intermediate **2** by PPh_3 is favored over trapping of **2** by Et_3SiH by 2 kcal/mol as shown by $\Delta\Delta H^\ddagger$. The ratio k_2/k_{-1} at 50°C is 7.3. Graham and Hart-Davis have found that for competitive trapping of **2** in heptane solution by PPh_3 and by Ph_3SiH , the ratio k_2/k_{-1} is 3.6 at 50°C .² From Wrighton and Hill's work, the relative rates of reaction of intermediate **2** with Ph_3SiH and with Et_3SiH are known to be 1.74–1.7. From these values, the expected ratio of k_2/k_{-1} for PPh_3 vs Et_3SiH is 6.3, in good agreement with our results.

Using time-resolved infrared spectroscopy Poliakoff et al. have determined the rate of reaction of $\text{CpMn}(\text{CO})_2$ with PPh_3 in heptane to be $k_2 = 4.2 \times 10^7 \text{ L}/(\text{mol}\cdot\text{s})$ at 53°C .²² From our values of $\Delta\Delta H^\ddagger$ and $\Delta\Delta S^\ddagger$, k_{-1} at 25°C from Table I, and the values of ΔH_{-1}^\ddagger and ΔS_{-1}^\ddagger derived from Wrighton's data, we calculate that $k_2 = 7 \times 10^7 \text{ L}/(\text{mol}\cdot\text{s})$ at 53°C . These values for k_2 agree remarkably well considering the differences in the methods used to obtain these values, as well as the indirect route required to calculate these quantities.

(21) Barbeau, C.; Dichmann, K. S.; Ricard, L. *Can. J. Chem.* **1973**, *51*, 3027–3031.

(22) Creaven, B. S.; Dixon, A. J.; Kelly, J. M.; Long, C.; Poliakoff, M. *Organometallics* **1987**, *7*, 2600–2605.

When heptane complex **2** is trapped by PPh_3 or Et_3SiH , the only slightly greater stabilization of the transition state by the incoming phosphine ligand in comparison to the stabilization provided by Et_3SiH is consistent with an early transition state with very little Mn-P bond formation. This suggests that the transition state has very little associative character. With a dissociative transition state, the overwhelming component to ΔH_{-1}^* is loss of the Mn-heptane interaction in **2**. Thus, the value for ΔH_{-1}^* provides a lower bound of approximately 8 kcal/mol for the magnitude of this interaction. We had previously estimated the Mn-heptane interaction in **2** to be approximately 8-9 kcal/mol by comparison of activation enthalpies and enthalpies of reaction for the substitution of *cis*-cyclooctene and dibutyl sulfide from $\text{CpMn}(\text{CO})_2\text{L}$ by phosphine and phosphite ligands.¹⁰ Both previous estimates and the estimate reported here, although in good agreement with one another, are in error to the degree that a residual Mn-heptane interaction exists in the transition state. Rayner's studies on metal-hydrocarbon interactions clearly show them to be in the 10-kcal/mol range.²³ As a consequence, we

believe that although the true Mn-heptane interaction may be somewhat greater than 8 kcal/mol, the difference is probably not substantial.

Finally, with the observation of a substantial Mn-heptane interaction in complex **2**, both the $\Delta H_{\text{Mn-CO}}$ and the ΔH_{-1} values reported here are smaller in magnitude than the corresponding gas-phase values. Thus, the gas-phase Mn-CO bond dissociation energy is then calculated to be 54.8 kcal/mol and the enthalpy of addition of Et_3SiH to $\text{CpMn}(\text{CO})_2$ is -28.1 kcal/mol.

Acknowledgment. We acknowledge the National Institutes of Health (Grant No. GM-42704) and the donors of the Petroleum Research Fund, administered by the American Chemical Society, for financial support of this research. D.M.H. acknowledges support from a U.S. Department of Education Fellowship Grant to the USC Chemistry Department. A.W.H. acknowledges partial support from an NSF-REU grant.

Supplementary Material Available: Listings of k_{obsd} at different $[\text{PPh}_3]$ and $[\text{Et}_3\text{SiH}]$ for the reaction of $\text{CpMn}(\text{CO})_2(\text{H})(\text{SiEt}_3)$ with PPh_3 in heptane solution at 35, 50, 60, 70, and 80 °C (2 pages). Ordering information is given on any current masthead page.

(23) (a) Ishikawa, Y.; Brown, C. E.; Hackett, P. A.; Rayner, D. M. *Chem. Phys. Lett.* **1988**, *150*, 506-510. (b) Brown, C. E.; Ishikawa, Y.; Hackett, P. A.; Rayner, D. M. *J. Am. Chem. Soc.* **1990**, *112*, 2530-2536.

Synthesis and Characterization of Trinuclear Iron(II) and Manganese(II) Carboxylate Complexes: Structural Trends in Low Valent Iron and Manganese Carboxylates

R. Lynn Rardin, Peter Poganiuch, Avi Bino,¹ David P. Goldberg, William B. Tolman, Shuncheng Liu, and Stephen J. Lippard*

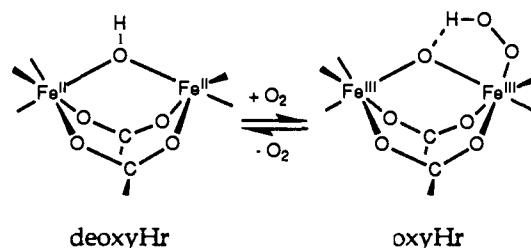
Contribution from the Department of Chemistry, Massachusetts Institute of Technology, Cambridge, Massachusetts 02139. Received December 20, 1991

Abstract: Reaction of $\text{Fe}(\text{O}_2\text{CCH}_3)_2$ or $\text{Mn}(\text{O}_2\text{CCH}_3)_2 \cdot 4\text{H}_2\text{O}$ with bidentate nitrogen donor ligands affords the trinuclear complexes $[\text{M}_3(\text{O}_2\text{CCH}_3)_6\text{L}_2]$ [$\text{M} = \text{Fe}$, $\text{L} = \text{BiPhMe}$ (**1**); $\text{M} = \text{Mn}$, $\text{L} = \text{BiPhMe}$ (**2**) or 1,10-phenanthroline (**3**)] in high yields. As judged from X-ray diffraction studies, these complexes adopt a novel linear structure, with one monodentate and two bidentate bridging carboxylates spanning each pair of metal atoms. Within this motif there are two geometric isomers that exist, designated "syn" or "anti" depending upon the orientation of the bidentate nitrogen donor ligands with respect to one another across the plane defined by the three metal atoms and the two monodentate bridging oxygen atoms. The bidentate and monodentate bridging modes are related by a carboxylate shift mechanism, proposed on the basis of observed variations in the interaction of the nonbridging, or dangling, oxygen atoms of the monodentate carboxylates with the terminal metal atoms. Such a carboxylate shift has recently been observed for the bridged dimetallic center in ribonucleotide reductase. Structural characterization of three isomers of compound **2** revealed a considerable degree of flexibility in the tricarboxylate-bridged dimetallic unit, with M...M distances ranging from 3.370 (**3**) to 3.715 (**2**) Å. From temperature-dependent magnetic susceptibility studies, compound **1** was found to be a ferromagnetically coupled triiron(II) complex with bridging oxygen atoms. A theoretical fit of the magnetic susceptibility data for **1** revealed the J value for ferromagnetic exchange coupling between adjacent iron atoms to be in the range +5 to +10 cm^{-1} . Magnetic susceptibility results for **2** revealed more typical antiferromagnetic coupling, with $J = -2.8$ (1) cm^{-1} for adjacent manganese atoms. The relevance of these results to the properties of carboxylate-bridged dimetallic iron and manganese centers in metalloproteins and the chemical reactivity of the complexes are briefly discussed.

Introduction

Proteins containing non-heme polyiron or polymanganese oxo units in their active centers, including hemerythrin (Hr), ribonucleotide reductase (RR), methane monooxygenase (MMO), purple acid phosphatase (PAP), the water oxidizing center of photosystem II (PSII), and ferritin, have been the subject of considerable investigation.²⁻¹⁶ For most of these proteins, redox

Scheme I



chemistry is involved in the key functional steps, with the metals cycling among the +2, +3, and +4 oxidation states. Whereas

(1) Permanent address: Department of Inorganic and Analytical Chemistry, Hebrew University of Jerusalem, 91904 Jerusalem, Israel.

(2) Lippard, S. J. *Angew. Chem., Int. Ed. Engl.* **1988**, *27*, 344.

(3) Que, L., Jr.; True, A. E. *Prog. Inorg. Chem.* **1990**, *38*, 97.

(4) Kurtz, D. M., Jr. *Chem. Rev.* **1990**, *90*, 585.

(5) Vincent, J. B.; Olivier-Lilley, G. L.; Averill, B. A. *Chem. Rev.* **1990**, *90*, 1447.